The Astronomical Journal, 160:250 (12pp), 2020 December https://doi.org/10.3847/1538-3881/abbad0

Recoverability of Known Near-Earth Asteroids

Javier Roa, Davide Farnocchia, Paul W. Chodas, Steven R. Chesley, Ryan S. Park, and Shantanu P. Naidu
Jet Propulsion Laboratory, California Institute of Technology 4800 Oak Grove Dr., Pasadena, CA 91109, USA; javier.roa@jpl.nasa.gov
Received 2020 July 14; revised 2020 September 21; accepted 2020 September 21; published 2020 November 6

Abstract

This paper analyzes the current population of known near-Earth asteroids (NEAs) and presents statistics on the recoverability of NEAs with both targeted observation campaigns and all-sky surveys. For an asteroid to be observable at a future apparition, given the right geometry, the plane-of-sky uncertainty must be small enough to be covered by a telescope's field of view and the asteroid must be brighter than the detector's limiting magnitude. Since recoverability is a telescope-dependent property, we select two representative instruments that span a wide range of capability and availability: the 1.0 m I52 telescope of the Catalina Sky Survey and the Hyper Suprime-Cam of the 8.2 m Subaru telescope. Based on this choice, we classify asteroids as recoverable, potentially recoverable, and not recoverable depending on whether they could be detected with an I52-class telescope, only with a Subaru-class telescope, or with neither, respectively. Using these definitions, we find that the majority (90%) of NEAs with $H < 22$ and most (93%) potentially hazardous asteroids are recoverable or potentially recoverable in the next 50 yr. When considering fainter asteroids down to $H \leqslant 28$, about two-thirds of the NEA population and half of the low minimum-orbit intersection distance (MOID) asteroids (MOID $\leqslant$ 0.05 au) are either recoverable or potentially recoverable. As of 2019 October 13, the Sentry risk list includes 193 objects with an impact probability greater than 10^{-6} that are not recoverable. The fraction of NEAs and low-MOID NEAs that are not recoverable can be reduced by up to 47% and 43%, respectively, when incorporating statistical estimates of serendipitous recoveries by all-sky surveys.

Unified Astronomy Thesaurus concepts: Near-Earth objects (1092); Sky surveys (1464); Solar system astronomy (1529); Asteroids (72)

1. Introduction

In 1998, motivated by the findings of the 1992 Spaceguard report (Morrison 1992), which assessed the magnitude of the threat posed by asteroid impacts with Earth, the U.S. Congress directed NASA to discover 90% of all near-Earth asteroids (NEAs) greater than 1 km in size (which is a proxy for the magnitude limit $H < 17.75$) by 2008. Multiple surveys including the Lincoln Near-Earth Asteroid Research (LINEAR) project (Stokes et al. 2000), the Catalina Sky Survey (Christensen 2019), the Panoramic Survey Telescope and Rapid Response System (Pan-STARRS; Kaiser et al. 2002), and the extended mission of the Wide-field Infrared Survey Explorer (WISE) spacecraft, NEOWISE (Mainzer et al. 2011), were funded to help meet this congressional directive.

Independent estimates of the population of NEAs larger than 1 km published in the last decade combined with the actual number of discoveries (901 as of 2019 October 13) confirm that the initial goal of detecting 90% of kilometer-sized NEAs has been fulfilled. Table 1 compares the current completion levels according to several population models, which range from 83% (Stuart & Binzel 2004) to 96% according to a more recent estimate by Stokes et al. (2017). Such population estimates rely on different sources of data and assumptions. For instance, when the NEOWISE team published the preliminary results of the survey (Mainzer et al. 2011), they estimated the population of NEAs larger than 1 km by extrapolating the rate of discoveries, arriving at 981 ± 19 NEAs. Harris & D'Abramo (2015) produced an independent estimate (990 ± 20) based on the ratio of detections of new asteroids to already known asteroids. Granvik et al. (2016) derived statistical conclusions from models that predict the migration of NEAs from the asteroid belt to the inner solar system and estimated the population of NEAs larger than 1 km at 1008 ± 45. Tricarico (2017) combined 20 yr of data from nine of the most prolific asteroid surveys and estimated the population at 920 ± 10 asteroids. The report by Stokes et al. (2017) combined and refined previous population models to produce a recalibrated estimate (934 NEAs).

The 1998 congressional mandate was extended in 2005 to become the Near-Earth Object Survey Act, which directed NASA to discover 90% of NEAs with $H < 22$ (larger than 140 m) by 2020.[1] The current number of discovered NEAs with $H < 22$ is 8662, resulting in approximately 35% completion according to the population estimate by Stokes et al. (2017). The development of more capable surveys like the Large Synoptic Survey Telescope (LSST; Ivezić et al. 2019) and dedicated missions like NEOCam (Mainzer et al. 2006) will greatly contribute to achieving the requested completion.

The initial discovery is only the first step toward a catalog of NEAs that is both current and complete. Once an object has been discovered, follow-up observations are required to refine the asteroid's orbit. Reducing the orbit uncertainty facilitates future observations and is critical for assessing the possibility of an impact on Earth. If the orbit uncertainty of a given asteroid grows too large over time or if the object becomes too faint, it might not be possible to redetect the asteroid in the future with targeted observation campaigns. At that point, the only option for recovery would be a potential serendipitous rediscovery by an all-sky survey. Serendipitous rediscoveries at several apparitions are common and reliable algorithms to produce orbit linkages are required to associate those observations with existing objects (Milani et al. 2000; Farnocchia et al. 2015).

When investigating the possibility of directly measuring the Yarkovsky effect on NEAs, Vokrouhlický et al. (2000)

[1] https://www.congress.gov/109/crpt/hrpt158/CRPT-109hrpt158.pdf

Table 1
Population Estimates of NEAs with $H \leqslant 17.75$ (Approximately Larger than 1 km) and Current Completion Levels as of 2019 October 13

Source	Estimate	Completion
Stuart & Binzel (2004)	1090 ± 180	83%
Mainzer et al. (2011)	981 ± 19	92%
Harris & D'Abramo (2015)	990 ± 20	91%
Granvik et al. (2016)	1008 ± 45	89%
Tricarico (2017)	920 ± 10	98%
Stokes et al. (2017)	934	96%

determined that follow-up observations at multiple apparitions are required to adequately constrain the orbital uncertainty. They identified asteroid 1998 KY_{26} as a promising candidate for detecting the Yarkovsky effect during its 2024 close approach with Earth although the orbit needed to be refined with careful follow-up. Tholen (2003) successfully recovered the asteroid in 2002, reducing the predicted orbital uncertainty during the 2024 encounter to a level that allows detection of the displacement caused by the Yarkovsky effect.

To determine whether an asteroid can be recovered at a future epoch, Boattini et al. (2007) proposed a figure of merit that accounts for the plane-of-sky uncertainty of the object, its Earth minimum-orbit intersection distance (MOID), the visual magnitude, and the evolution of the brightness. They established a priority list[2] to identify the objects that should be prioritized for follow-up. Previous work by Ostro et al. (2002) analyzed the opportunities for Earth-based recoveries (based on a visual magnitude cutoff) of several NEAs that had already been imaged with radar.

Even when the goal of discovering a prescribed fraction of the total NEA population is achieved, the question of what fraction of those NEAs can be recovered in the future still remains. Motivated by this fact, the present paper evaluates the performance of ongoing follow-up efforts by assessing the recoverability of known NEAs from a statistical perspective. First, we define three categories in which to classify all known NEAs with $H \leqslant 28$ (approximately larger than 10 m) depending on the capabilities of representative telescopes that could be used for recovery. The proposed categories are: recoverable (a routine recovery is possible), potentially recoverable (an aggressive recovery campaign is required), and not recoverable. Next, we propagate the orbits of the entire population of known NEAs forward into the future and simulate the observability conditions of each asteroid. We then assign each NEA to one of the three categories and analyze the resulting distribution. Special attention is paid to identifying the nonrecoverable NEAs that appear on the Sentry risk list,[3] which presents asteroids of all sizes that admit Earth-impact trajectories within the orbital uncertainty.

2. Recovery Statistics

2.1. Definitions

The evolution of the orbit uncertainty and the brightness of an object are the main factors determining the success of targeted observation campaigns. To predict the plane-of-sky uncertainty for an optical observation at a given date, we propagate the orbital uncertainty and compute the semimajor axis of the 1σ covariance ellipse projected on the plane of the sky (σ_{pos}). The initial distribution of orbital uncertainty is determined following the weighting scheme proposed by Vereš et al. (2017). The force model is described in detail by Farnocchia et al. (2015) and includes the Newtonian gravitational perturbations from all the planets, Pluto, the Moon (using JPL's DE431 ephemerides, see Folkner et al. 2014), and the 16 most massive asteroids in the solar system. The contribution from the general relativistic effects for the Sun is modeled using the formulation by Damour & Deruelle (1985). The uncertainty σ_{pos} and the visual magnitude (V) are recorded at one-day intervals. An adequate observation geometry requires that the solar elongation ε be large enough, which we conservatively limited to $\varepsilon > 60°$. For simplicity we only consider geocentric observing parameters, and ignore constraints due, for example, to the geocentric latitude/longitude of the observatory. This simplification eliminates the dependency on the observer topocentric location and, except for the case of objects that are very close to Earth, the effect on the predicted size of the plane-of-sky uncertainty is small. Additional simplifications to reduce the dimension of the space of parameters include assuming perfect weather conditions and that the exposure time is enough to reach a prescribed magnitude threshold. Different observability conditions might be applicable with space-based telescopes placed, for example, at the Sun–Earth L_1 equilibrium point, on a geosynchronous orbit, or describing a Venus-trailing orbit (Stokes et al. 2017).

Based on the time history of ε, σ_{pos}, and V, asteroids are classified into one of the following categories.

1. *Recoverable*. The asteroid can be detected at least one night using a telescope with the capabilities of the 1.0 m I52 telescope of the Catalina Sky Survey (Christensen 2019), which imposes the constraints $\pm 3\sigma_{\text{pos}}$ within 34.′3 and $V < 22$. This set of constraints simulates routine recoveries and only considers detections in a single field of view, that is, without mosaicking.
2. *Potentially recoverable*. The asteroid cannot be detected with an I52-class telescope but it can be detected at least once with a telescope comparable to Subaru provided with the Hyper Suprime-Cam ($\pm 3\sigma_{\text{pos}}$ within 90′ and $V < 27$; Miyazaki et al. 2012). The magnitude limit in this category approximately captures the faintest objects that can be detected with today's instruments. Resorting to a Subaru-class telescope indicates an aggressive effort to recover the asteroid, which has to take into account the limited availability of such telescopes.
3. *Not recoverable*. The asteroid cannot be detected with either I52-class or Subaru-class telescopes.

Given the superior capabilities of Subaru-class telescopes, both in terms of field of view and limiting magnitude, the asteroids that can be detected with I52-class telescopes are a subset of those that can be detected with the capabilities of Subaru. The three classes defined above are mutually exclusive.

Taking asteroid (99942) Apophis as an example simply to show how the proposed classification works in practice, Figure 1 illustrates how the plane-of-sky uncertainty and the visual magnitude evolve over time and how they relate to the constraints derived from the capabilities of the two reference telescopes. Each data point corresponds to one night of observation. Prior to the 2029 close approach with Earth and through the end of the year,

[2] http://neo.ssa.esa.int/priority-list
[3] https://cneos.jpl.nasa.gov/sentry/

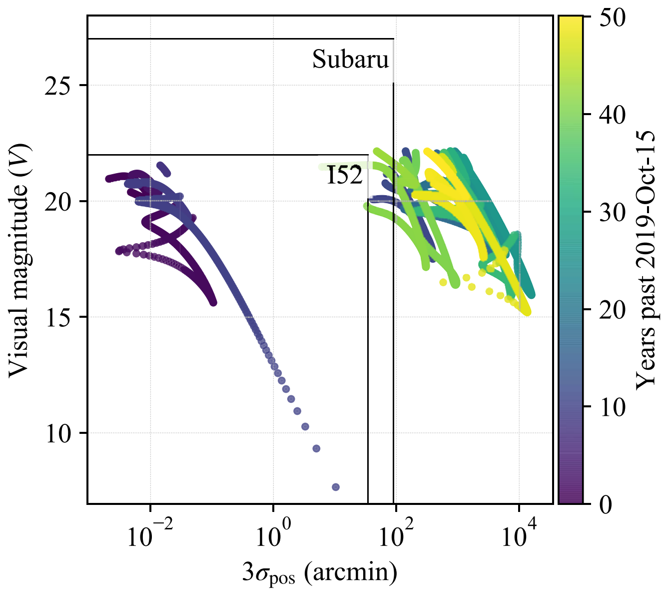

Figure 1. Time evolution of the plane-of-sky uncertainty and the visual magnitude of asteroid (99942) Apophis. The boxes represent the upper bounds on σ_{pos} and V for each reference telescope. Only the data points with $\varepsilon > 60°$ are shown.

the 3σ plane-of-sky uncertainty is smaller than 6′ and the object is bright enough to be recovered by an I52-class telescope. There are many observation opportunities within this period, as shown by the number of data points that fall inside the I52-class box. Since there are observing opportunities within the capabilities of I52 and based solely on the data that is currently available, this particular asteroid is classified as recoverable. It is worth noting that the rapid growth of the uncertainty observed in the figure is caused by the close approach in 2029 April, which results in a strong divergence of the dynamics (Farnocchia et al. 2013).

2.2. The Population of Known NEAs

There are currently[4] 21,069 NEAs in the JPL Small Body Database with absolute magnitudes ranging from 9.5 for (1036) Ganymed to 33.2 for 2008 TS_{26}. In the present paper, we limit the analysis to the 20,539 NEAs with $H \leqslant 28$. The number of known NEAs that satisfy $H \leqslant 17.75$ (approximately larger than 1 km) is 901, and 8662 NEAs have $H < 22$ (approximately 140 m). Among the current population of NEAs with $H \leqslant 28$, there are 9497 asteroids with Earth MOID lower than 0.05 au, which include the 1983 objects that are classified as potentially hazardous asteroids[5] (PHAs). When limiting the absolute magnitude to $H \leqslant 28$, there are 331 asteroids on the Sentry risk list with maximum impact probability (IP) greater than 10^{-6} and 507 with IP $> 10^{-7}$.

Figure 2(a) presents the number of NEAs that are recoverable, potentially recoverable, and not recoverable in the next 50 years binned by absolute magnitude. The width of each bin is $\Delta H = 0.5$. Table 2 indicates the relative fractions, both per magnitude level and cumulative. In total, 74% of objects with $H < 22$ are recoverable, 16% are potentially recoverable, and 10% are not recoverable. The fraction of recoverable NEAs with $H \leqslant 28$ is 36%, 25% are potentially recoverable, and 39% are not recoverable.

The distributions of low-MOID NEAs in each category (recoverable, potentially recoverable, and nonrecoverable) shown in Figure 2(b) are centered at smaller asteroid sizes (or equivalently at larger H values) compared to the corresponding distributions of NEAs in Figure 2(a). This is due to the fact that low-MOID asteroids come closer to Earth and tend to be brighter for a given size, which facilitates the discovery of smaller asteroids. Almost half of all low-MOID asteroids are not recoverable. Conversely, PHAs are relatively large by definition ($H < 22$) and most are recoverable (83%); only 7% are not recoverable while 10% are potentially recoverable.

Asteroids on the Sentry risk list tend to be small and have short data arcs leading to relatively large initial orbit uncertainties, which is why impacts cannot be ruled out yet, and, consequently, the number of nonrecoverable objects dominates the statistics within almost every H bin. From the 331 NEAs with $H \leqslant 28$ that present virtual impactors with IP $> 10^{-6}$, 58% are not recoverable in the next 50 years. According to Table 2, there are three objects on the Sentry list with IP $> 10^{-6}$ and $H < 22$; they are asteroids (29075) 1950 DA (Farnocchia & Chesley 2014), (99942) Apophis (Vokrouhlický et al. 2015), and (101955) Bennu (Chesley et al. 2014), which are all recoverable.

One might ask how these results would change if the timescale for recovery is shorter than 50 years, or longer. Table 3 compares how the distribution of recoverable, potentially recoverable, and nonrecoverable asteroids changes when considering recoveries in the next 20, 50, and 100 years. Over 60% of all NEAs could be recovered in the next 50 years using I52-class and Subaru-class telescopes, whereas 39% of the orbits are not recoverable under the assumptions of this study. If the recovery window is extended to 100 years, the fraction of nonrecoverable NEAs goes down to 36%. The fraction of low-MOID NEAs that are not recoverable is higher because, on average, known objects of this class are smaller (see Figure 2(b)), with up to 49% of the population not being recoverable in the next 50 years. The fraction of recoverable and potentially recoverable asteroids increases by approximately 10% when extending the time span from 20 to 50 years as well as from 50 to 100 years.

Based on the results from Figure 2, Figure 3 shows the fraction of asteroids that are recoverable, potentially recoverable, and not recoverable in the next 50 years within each H bin, together with the cumulative fraction of asteroids in each category. For $H \geqslant 22$, the relative fraction of potentially recoverable NEAs per bin becomes greater than the fraction of recoverable asteroids. For $H \geqslant 23.5$, the relative fraction of asteroids that are not recoverable dominates the per bin distribution.

To better understand the statistics and outliers, we set an arbitrary magnitude limit at $H < 19$ and analyzed all the asteroids that are potentially recoverable and not recoverable. Table 4 lists the asteroids with $H < 19$ that are either potentially recoverable (34 NEAs, four low-MOID, none from Sentry) or not recoverable (42 NEAs, seven low-MOID, none from Sentry) in the next 50 years. Large low-MOID asteroids discovered in the last 10 years can all be recovered or potentially recovered except for the case of 2015 BO_{519}. This asteroid was discovered in 2015 January by the Kepler space telescope[6] when the asteroid was not observable from Earth

[4] Data retrieved on 2019 October 13.
[5] MOID $<$ 0.05 au, $H < 22$.
[6] Minor Planet Circulars Supplement 747529, 2016 December 5.

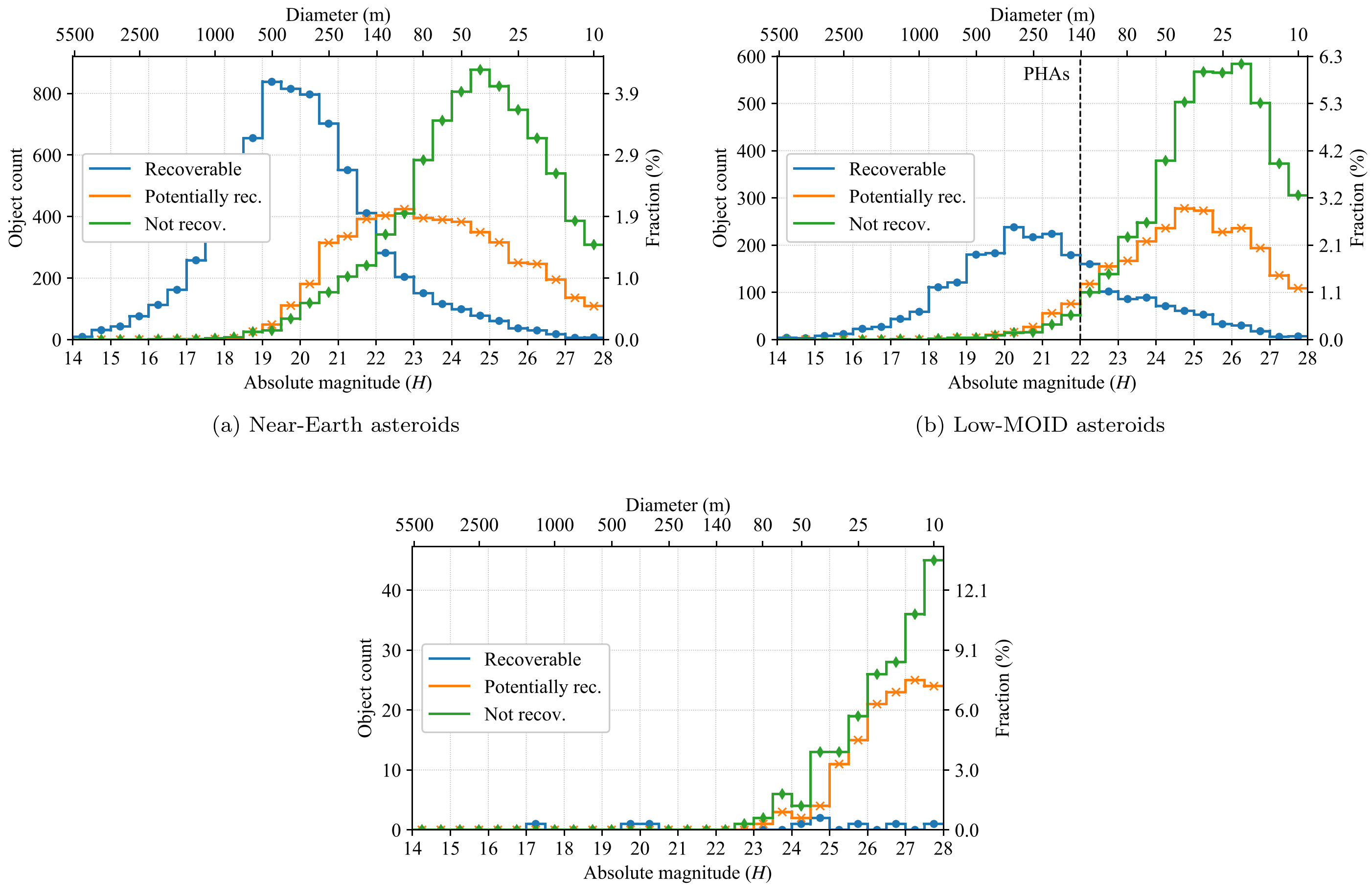

(a) Near-Earth asteroids

(b) Low-MOID asteroids

(c) Sentry risk list (IP $> 10^{-6}$)

Figure 2. Number of recoverable, potentially recoverable, and nonrecoverable asteroids distributed by absolute magnitude. The conversion to diameter assumes an albedo of 0.14. The last bin includes asteroids with $27.5 \leqslant H \leqslant 28$.

and therefore no follow-up was possible. Only three nights of data are available. The lack of follow-up observations results in a large plane-of-sky uncertainty that prevents a targeted recovery.

In general, asteroids that are not recoverable have short data arcs of just a few days. Exceptions to this rule are asteroids (418265) and 2019 AQ_3, whose data arcs span several years. They are both members of the Atira group, which means that their orbits are completely interior to Earth's orbit. Thus, it is the constraint on the solar elongation $\varepsilon > 60°$ that makes these two asteroids not recoverable. Figure 4(a) depicts the orbit of (418265) in the Sun–Earth rotating frame in the next 50 years, producing a torus centered at the Sun. The external diameter of the torus and ultimately the maximum solar elongation depend on the aphelion distance, which in this case results in a maximum solar elongation of only 55°. The orbit of 2019 AQ_3 is qualitatively similar, with a maximum solar elongation of 52°. Despite not being recoverable, it should be noted that these asteroids pose no impact risk because their orbits remain interior to Earth's. Furthermore, such objects could be recovered with targeted follow-up, which can go down to lower solar elongations. Twilight surveys like the one recently conducted with the Zwicky Transient Facility (Ye et al. 2020) can help recover these two objects serendipitously.

Asteroid 2015 KC_{19} stands out as an outlier in terms of length of the data arc compared to the rest of objects on the list of potentially recoverable (Table 4(a)). The orbital period is approximately 3.5 years, revealing that the asteroid is close to a 7:2 resonance with Earth. The effect of this resonance can be appreciated in the orbit plot in Figure 4(b). If the asteroid were trapped in the resonance, the orbit would be periodic in the rotating frame and the observation conditions would repeat every seven years. Therefore, no improvements in the observability conditions should be expected after the first complete period. In reality, this configuration is unstable and the orbit of the asteroid drifts over time in the rotating frame, regressing at a rate of 1.6 deg/year. The point of closest approach to Earth moves farther away from Earth for the next 50 years, not facilitating the asteroid's recovery. Even though the point of closest approach per cycle might come closer to Earth after 50 years, the orbit uncertainty will be too large for detection. The high inclination of this asteroid keeps it generally distant from Earth even when it is on the same side of the Sun as Earth, making detection more difficult.

The evolution of the plane-of-sky uncertainty and visual magnitude of 2015 KC_{19} (Figure 5) indicates that initially, when the uncertainty is small, the asteroid is too faint to be detected by I52-class telescopes. As time progresses, the uncertainty describes 3.5 year cycles reaching its maximum value at perihelion, where the object is brightest but the uncertainty is too large for recovery even with the capabilities of Subaru. In addition, the uncertainty grows larger after each cycle. This phenomenon combined with the elongation

Table 2
Fraction of Asteroids that are Recoverable ("Rec."), Potentially Recoverable ("Pot."), and Not Recoverable ("Not") in the Next 50 yr

(a) Near-Earth asteroids

		Current Bin (%)			Cumulative (%)		
H_{bin}	N_{bin}	Rec.	Pot.	Not	Rec.	Pot.	Not
<16	173	100.0	0.0	0.0	100.0	0.0	0.0
[16, 17)	278	98.9	0.0	1.1	99.3	0.0	0.7
[17, 18)	619	98.5	0.5	1.0	98.9	0.3	0.8
[18, 19)	1277	95.0	2.4	2.6	96.8	1.4	1.8
[19, 20)	1911	86.5	8.4	5.1	92.2	4.6	3.3
[20, 21)	2268	66.1	21.9	12.0	83.1	10.6	6.3
[21, 22)	2136	45.0	34.1	20.9	73.7	16.4	9.9
[22, 23)	2065	23.5	40.0	36.4	64.1	20.9	15.0
[23, 24)	2348	11.4	33.4	55.2	54.6	23.2	22.2
[24, 25)	2592	6.8	28.2	64.9	46.7	24.0	29.3
[25, 26)	2235	4.4	25.3	70.3	41.4	24.2	34.4
[26, 27)	1684	2.9	26.2	71.0	38.1	24.3	37.6
[27, 28]	953	1.4	25.7	72.9	36.4	24.4	39.2

(b) Low-MOID Asteroids

		Current Bin (%)			Cumulative (%)		
H_{bin}	N_{bin}	Rec.	Pot.	Not	Rec.	Pot.	Not
<17	77	100.0	0.0	0.0	100.0	0.0	0.0
[17, 18)	104	99.0	0.0	1.0	99.4	0.0	0.6
[18, 19)	242	95.9	1.7	2.5	97.4	0.9	1.7
[19, 20)	390	93.1	3.6	3.3	95.3	2.2	2.5
[20, 21)	529	86.0	8.1	5.9	91.7	4.5	3.8
[21, 22)	619	65.1	21.3	13.6	83.3	9.8	6.9
[22, 23)	774	33.9	35.3	30.9	69.3	17.0	13.7
[23, 24)	1015	17.2	36.9	45.8	55.2	22.4	22.4
[24, 25)	1528	8.6	33.6	57.7	41.7	25.7	32.6
[25, 26)	1719	5.0	29.1	65.9	32.7	26.5	40.8
[26, 27)	1563	3.1	27.5	69.4	27.3	26.7	46.0
[27, 28]	937	1.4	26.1	72.5	24.7	26.7	48.6

(c) Sentry Risk List (IP $> 10^{-6}$)

		Current Bin (%)			Cumulative (%)		
H_{bin}	N_{bin}	Rec.	Pot.	Not	Rec.	Pot.	Not
<22	3	100.0	0.0	0.0	100.0	0.0	0.0
[22, 23)	1	0.0	0.0	100.0	75.0	0.0	25.0
[23, 24)	12	0.0	33.3	66.7	18.8	25.0	56.2
[24, 25)	26	11.5	23.1	65.4	14.3	23.8	61.9
[25, 26)	59	1.7	44.1	54.2	6.9	35.6	57.4
[26, 27)	99	1.0	44.4	54.5	4.0	40.0	56.0
[27, 28]	131	0.8	37.4	61.8	2.7	39.0	58.3

Note. For each absolute-magnitude bin, the table provides the number of asteroids in the bin (N_{bin}) and both the per bin and cumulative percentages.

constraint is responsible for the asteroid being only potentially recoverable.

In general, the effect of the constraint $\varepsilon > 60°$ on the overall statistical results is small. Relaxing this constraint to $\varepsilon > 45°$, for example, increases the number of potentially recoverable NEAs by 135 (3% of the current tally), and the number of recoverable NEAs by 21 (0.3% increase). Under this assumption, of the 76 nonrecoverable objects with $H < 19$ identified in Table 4, asteroids (418265), 2019 LF_6, and 2019 AQ_3, which are members of the Atira group, would become recoverable. Asteroids 2011 CN_2, 2009 TE_{10}, and 2011 LD_1 are members of the Apollo group and would become potentially recoverable.

2.3. Recovery of NEAs with H < 22

The number of NEA discoveries started rising significantly in 1998 following the mandate from U.S. Congress to detect 90% of NEAs with diameters greater than 1 km. Figure 6 displays the number of recoverable, potentially recoverable, and nonrecoverable NEAs with $H < 22$ distributed by discovery year. The initial phase of rapid discovery of the objects that were visible at the time leads to a large number of recoverable orbits. Earlier discoveries generally had more time for arc extension and follow-up (even serendipitous), while more recent objects are more likely to only rely on follow-up during the discovery apparition. In addition, earlier discoveries tended to be the larger, 1 km, objects, which have been comparatively easier to recover. The number of discoveries of asteroids that are potentially recoverable has been growing steadily in the last 10 years while the number of per year discoveries of recoverable and nonrecoverable asteroids remained relatively constant. On the other hand, the fact that the total number of discoveries grows over time while the number of nonrecoverable objects remains approximately constant indicates an improvement in the performance of follow-up campaigns.

2.4. Follow-up Performance Over Time

The orbit uncertainty is strongly dependent on the length of the data arc that is available to produce an orbit fit. The shorter the data arc, the larger the initial uncertainty will be, and therefore the chances of the asteroid not being recoverable will increase. This is the reason why follow-up observations are critical when exploring recovery opportunities. To study the importance of the arc length on recoverability, we plotted the length of the data arc as a function of the discovery year for all recoverable, potentially recoverable, and nonrecoverable NEAs with $H \leqslant 28$ (see Figure 7).

Recoverable asteroids exhibit the longest data arcs consistent with small uncertainties. In fact, the data-arc span is typically comparable to the maximum possible span of the data arc defined as the number of days from discovery to today's date, which is indicated by a solid black line on the figure. The data arc of asteroids discovered from the 1970s to the late 1990s (before the increased rate of detections following the congressional mandate) is particularly close to the maximum value. These objects are typically numbered asteroids with favorable observational geometries, which are observed regularly. Later discoveries show more variability in the relative arc length but the more densely populated region is close to the maximum possible data-arc span. Most objects discovered before the year 2000 are recoverable and the 95th percentile corresponds to a data-arc length of 31 years.

In general, potentially recoverable asteroids have shorter data arcs than recoverable asteroids. Furthermore, the data arc of potentially recoverable asteroids discovered in the early 2000s is very short compared to the total number of nights available. Some asteroids discovered in recent years have long data arcs and yet they are potentially recoverable instead of recoverable. Most of these objects would become recoverable if the recovery window were extended beyond 50 years. Improvements in follow-up campaigns produced a slight upward trend in the length of the data arc of recent discoveries, which progressively gets closer to the maximum completeness of the data arcs. Still, the arc span is not enough to constrain the

Table 3
Number of Known NEAs, Low-MOID Objects (MOID < 0.05 au), and Asteroids on the Sentry Risk List with IP $> 10^{-6}$ That are Recoverable, Potentially Recoverable, and Not Recoverable (Catalog Retrieved on 2019 October 13)

		Next 20 yr		Next 50 yr		Next 100 yr	
Known NEAs	Recoverable	6992	34.0%	7474	36.4%	7706	37.5%
	Potentially Recoverable	4972	24.2%	5014	24.4%	5459	26.6%
	Not Recoverable	8575	41.8%	8051	39.2%	7374	35.9%
	Total	20539	⋯	20539	⋯	20539	⋯
Low MOID (<0.05 au)	Recoverable	2057	21.6%	2349	24.7%	2467	26.0%
	Potentially Recoverable	2342	24.7%	2531	26.7%	2906	30.6%
	Not Recoverable	5098	53.7%	4617	48.6%	4124	43.4%
	Total	9497	⋯	9497	⋯	9497	⋯
Sentry (IP $> 10^{-6}$)	Recoverable	9	2.7%	9	2.7%	10	3.0%
	Potentially Recoverable	110	33.3%	129	39.0%	138	41.7%
	Not Recoverable	212	64.0%	193	58.3%	183	55.3%
	Total	331	⋯	331	⋯	331	⋯

Note. The absolute magnitude is limited to $H \leqslant 28$ (diameter approximately larger than 10 m).

uncertainty to a level that is detectable with the capabilities of I52. By the time an asteroid is bright enough ($V < 22$), the orbit uncertainty will be too large. There are seven asteroids that present only one night of data but still fall within the detection capabilities of Subaru-class telescopes. The 95th percentile is 174 days.

The shortest arcs correspond to nonrecoverable asteroids. The longest data arcs of nonrecoverable asteroids typically remain below 100 days even for recent discoveries. There are four clear outliers in the bottom panel of Figure 7: asteroids (418265) and 2019 AQ_3, which have already been identified in Table 4; asteroid 2002 AA_{29}, which co-orbits with Earth causing the solar elongation to remain below 60°; and asteroid 2009 SQ_{103}, which cannot be recovered even with the capabilities of Subaru due to the unfavorable evolution of its orbital uncertainty and magnitude. In total, 1.5% of the 8051 NEAs that are not recoverable are single-night detections. The 95th percentile is 38 days.

The median data-arc span for NEAs that are recoverable, potentially recoverable, and not recoverable is 8.1 years, 31 days, and 8 days, respectively. In practice, this means that asteroids observed at more than one apparition are usually recoverable, objects observed for a relatively long period of time at a single apparition may be recovered with a Subaru-class telescope, whereas just a few nights of data at a single apparition are typically not enough for recovery, even with the capabilities of Subaru.

2.5. Date of Recovery

The date of recovery appears only indirectly in the classification criteria, when limiting the propagation of the orbit uncertainty and the visual magnitude. Figure 8 summarizes the results of a dedicated investigation of the influence of the date of discovery, which reveal that 85% of recoverable asteroids are detectable in the next 10 years (i.e., through 2030). Furthermore, the distribution of detections by date flattens quickly and exhibits a small residual toward the tail of the distribution corresponding to objects that will still not have been detected after 100 years. There are 37 recoverable and 90 potentially recoverable asteroids that will be redetected for the first time between 2110 and 2120. Furthermore, there are objects that will become observable with the capabilities of I52 after more than 100 yr into the future. These objects are likely close to low resonances that cause their orbits to drift slowly relative to Earth's, meaning that it will take hundreds of years for the perihelion of the asteroid to come close to Earth and for the object to become observable.

2.6. Distribution by Orbit Uncertainty

The uncertainty parameter U is a scalar indicator defined by the Minor Planet Center[7] that quantifies the uncertainty of an orbit solution. It ranges from zero (very small uncertainty) to nine (extremely large uncertainty). Since the orbital uncertainty is one of the major factors driving the recoverability of an object, we investigated the distribution of recoverable, potentially recoverable, and nonrecoverable NEAs by uncertainty parameter and presented the results in Figure 9(a). The results in the figure suggest that most NEAs with $U < 5$ are recoverable, NEAs with $5 \leqslant U < 7$ are usually potentially recoverable, and NEAs with $U \geqslant 7$ tend to be nonrecoverable. Combining the distributions of recoverable, potentially recoverable, and nonrecoverable asteroids in Figure 9(a) results in a bimodal distribution, with two modes at $U = 0$ and $U = 8$. The distributions of recoverable and potentially recoverable asteroids show bimodal characters too: the former has two modes at $U = 0$ and $U = 4$ and the latter at $U = 0$ and $U = 6$.

The uncertainty in semimajor axis is equivalent to the uncertainty in orbital period, which usually dominates the evolution of the plane-of-sky uncertainty. Figure 9(b) shows the distribution of recoverable, potentially recoverable, and nonrecoverable NEAs by their uncertainty in semimajor axis. The distribution is qualitatively similar to the distribution by uncertainty parameter, producing a combined distribution that is bimodal with modes at approximately 10^{-8} and 10^{-2} au. The results in Figure 9(b) corroborate that the distributions of recoverable and potentially recoverable asteroids are also bimodal.

The plane-of-sky uncertainty has been computed using the weighting scheme from Vereš et al. (2017), which is derived from statistics from prolific surveys. If the quality of the

[7] https://minorplanetcenter.net/iau/info/UValue.html

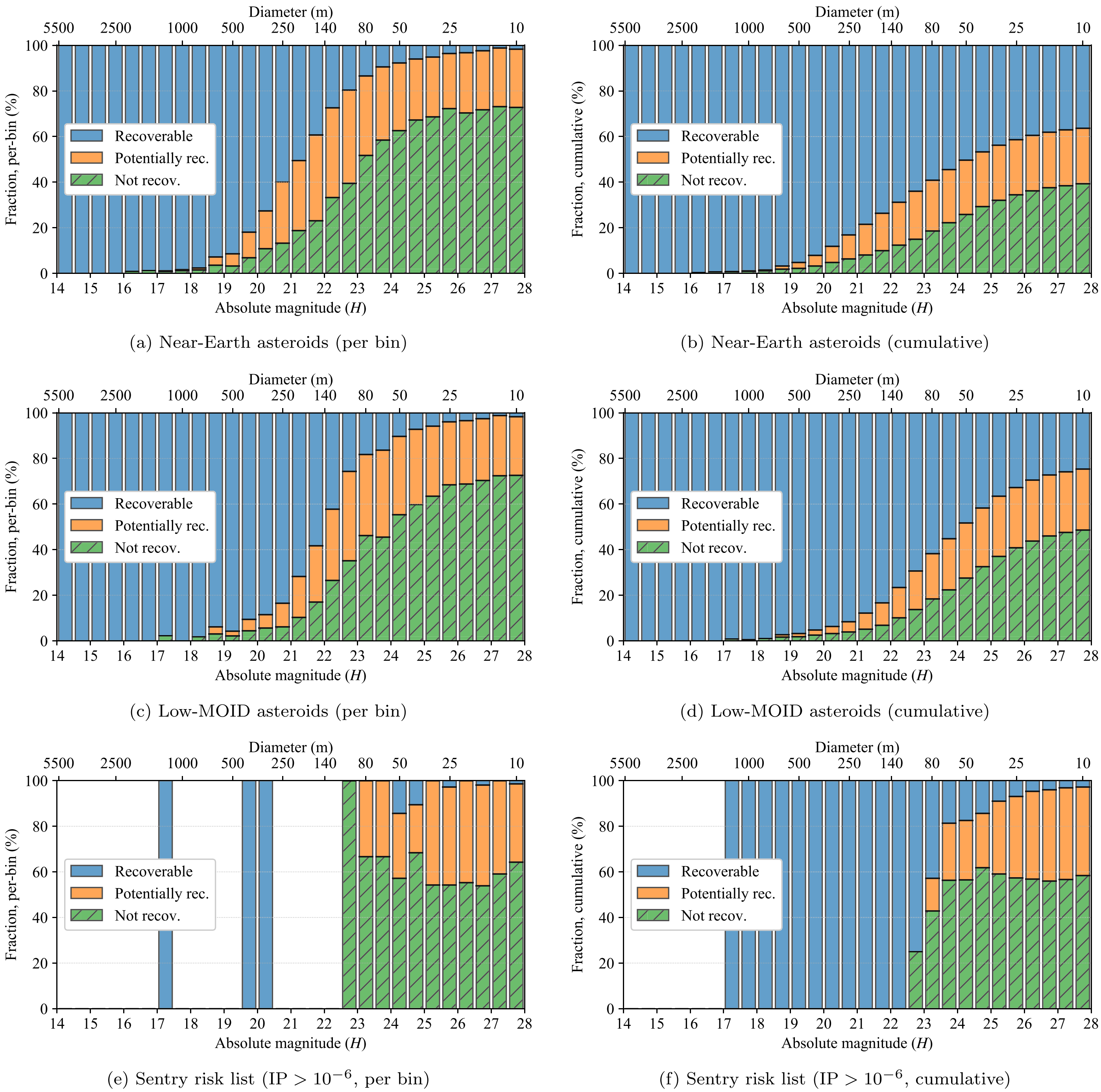

(a) Near-Earth asteroids (per bin)

(b) Near-Earth asteroids (cumulative)

(c) Low-MOID asteroids (per bin)

(d) Low-MOID asteroids (cumulative)

(e) Sentry risk list (IP $> 10^{-6}$, per bin)

(f) Sentry risk list (IP $> 10^{-6}$, cumulative)

Figure 3. Fraction of recoverable, potentially recoverable, and nonrecoverable asteroids relative to the total number of known objects inside each H bin and cumulative.

astrometric data improved, the uncertainty would be reduced and the distribution of recoverable, potentially recoverable, and nonrecoverable asteroids could change. To assess the impact that improving the quality of the data has on the statistical results presented in this paper, we recomputed the number of objects that can be detected with I52- and Subaru-class telescopes having reduced the plane-of-sky uncertainty by a factor of 2, which is consistent with a reasonable improvement in astrometric quality compared to the weighting by Vereš et al. (2017). The number of objects that can be detected with I52- and Subaru-class telescopes increased by 3% and 9%, respectively. Reducing the uncertainty even further by a factor of 5 (simulating a substantial improvement in the data) results in a 10% and a 21% increase, respectively. Improving the quality of the data is always desirable, although increasing the length of the data arc when possible has a more dramatic effect—particularly for uncertain orbits—since it can reduce the ephemeris uncertainty by orders of magnitude and secure the orbit for longer periods of time.

3. Serendipitous Recoveries

Even if the orbit uncertainty becomes too large for an asteroid to be recoverable according to the criteria in Section 2.1, the

Table 4
Potentially Recoverable and Nonrecoverable NEAs with $H < 19$. PHAs Are in Bold

(a) Potentially Recoverable

Designation	H	Arc (d)
2013 LH_{25}	17.3	86
2017 AQ_{20}	17.7	101
2017 WX_{14}	17.9	109
2016 WJ_8	18.1	67
A/2019 Q_2	18.2	39
2013 RD_{21}	18.2	32
2015 KC_{19}	18.4	439
2018 KK_2	18.4	84
2016 CB_{32}	18.5	114
2018 VG_1	18.5	15
2019 QC_8	18.6	25
2009 FA	18.6	29
2016 CB_{136}	18.6	20
2018 EP_1	18.6	21
2009 RZ_3	18.7	41
2014 DD_{80}	18.7	35
2017 KQ_{34}	18.7	25
2017 UA_5	18.7	21
1999 VX_{15}	18.8	40
2014 DD_{10}	18.8	34
2015 FW_{35}	18.8	31
2017 JT_2	18.8	24
2017 NM_6	18.8	122
2017 SR_{17}	18.8	32
2017 UZ_{42}	18.8	79
2018 UD	18.8	27
2019 MA_2	18.9	23
2009 CZ_2	18.9	72
2010 CV_{180}	18.9	62
2014 JQ_{57}	18.9	47
2018 HR_3	18.9	22
2018 SK_3	18.9	52
2018 TB_4	18.9	74
2019 GG_5	18.9	29

(b) Not Recoverable

Designation	H	Arc (d)
(418265)	16.4	3126
2010 HY_{22}	16.5	3
2010 GD_{37}	16.7	4
1999 XS_{35}	17.2	88
2019 LF_6	17.2	25
2019 AQ_3	17.6	1199
2007 AC_{12}	17.8	61
2014 MR_{26}	17.8	6
2016 RR_{20}	17.8	36
2005 GV_{190}	18.0	11
2005 JF_{108}	18.1	1
2015 BO_{519}	18.1	3
2015 GO	18.2	1
2016 RL_{41}	18.3	5
2001 VB	18.4	7
2011 KJ_{20}	18.4	6
2017 SH_{33}	18.4	1
1998 WR_5	18.5	28
2004 XF_{35}	18.5	31
1979 XB	18.6	4
2003 OC_3	18.6	41
2009 VQ_{25}	18.6	3
2011 CN_2	18.6	30
2014 JY_{79}	18.6	1
2007 JF_{16}	18.7	14
2012 KE_{25}	18.7	26
2016 NV_{38}	18.7	4
2014 TV_{81}	18.7	6
2001 CA_{21}	18.8	2
2000 KP_{44}	18.8	16
2006 LA	18.8	1
2009 TE_{10}	18.8	42
2011 LD_1	18.8	22
2014 WC_7	18.8	12
2015 BJ_{528}	18.8	37
2016 KS_3	18.8	6
2016 WQ_{55}	18.8	1
2017 SM_{33}	18.9	2
2007 AB_{12}	18.9	40
2008 GQ_3	18.9	29
2014 YT_{14}	18.9	19
2017 YX_8	19.0	3

asteroid might be detected serendipitously by an all-sky survey that scans the night sky systematically. Such survey detections can be modeled statistically by seeking asteroids that are bright enough (e.g., $V < 21.5$ based on Pan-STARRS1; Ramanjooloo et al. 2018) under favorable geometric conditions. In this study, we limit the solar elongation to $\varepsilon > 120°$. These simplified constraints implicitly assume that the simulated survey covers the entire sky nightly and they do not account for weather conditions or any other practical limitation. For this reason, our results are to be considered as an upper bound to the number of serendipitous discoveries. It should be noted that LSST will be able to detect objects down to the 24th magnitude (Jones et al. 2018), which means that fainter objects could be detected by the survey.

Table 5 indicates that 70% of NEAs could be recovered by all-sky surveys in the next 50 years instead of relying on targeted observations. More in particular, 47% of all NEAs that are not recoverable using the reference telescopes could be detected by surveys. Therefore, combining dedicated observations with all-sky surveys could reduce the fraction of nonrecoverable NEAs from 39% (Table 3) to 21%. Similarly, the fraction of nonrecoverable low-MOID asteroids could be reduced from 49% to 28%. Statistically, all-sky surveys could recover up to two-thirds of all potentially recoverable objects. More than one-third (37%) of the asteroids from the Sentry risk list that are not recoverable could be detected by surveys. Extending the recovery time window increases the chances of a serendipitous recovery as asteroids have more time to evolve and eventually cross the detection threshold. The results in Table 5 prove that surveys that continuously cover the night sky are a valuable source of orbit recoveries because they are not limited by the growth of the orbit uncertainty.

4. Impact Risk of Nonrecoverable Asteroids

4.1. Evolution of the MOID

A small MOID with respect to Earth is a necessary although not sufficient condition for an asteroid to potentially impact Earth. Thus, monitoring the time evolution of the MOID, which may change significantly due to planetary encounters with

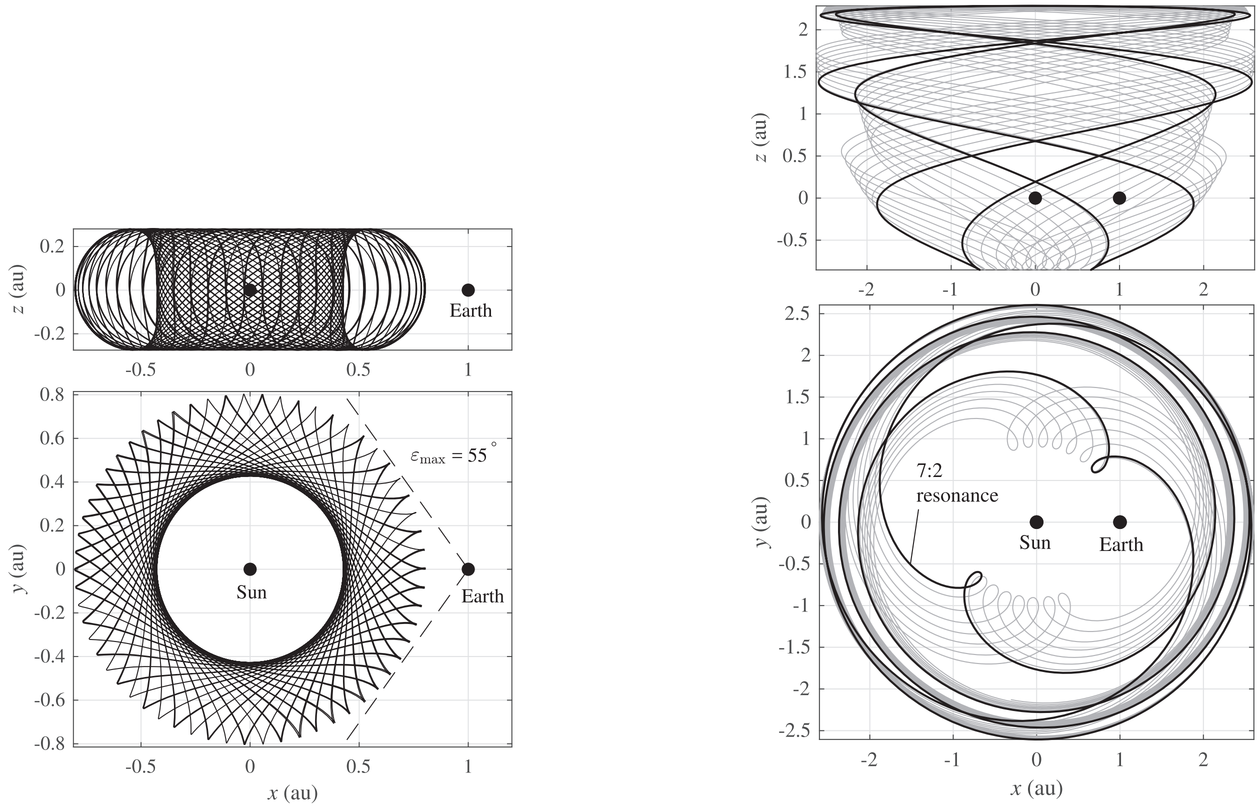

(a) Asteroid (418265)

(b) Asteroid 2015 KC_{19}. The black line corresponds to the exact 7:2 resonance and the gray line represents the actual orbit of the asteroid.

Figure 4. Orbits of asteroids (418265) and 2015 KC_{19} in the Sun–Earth rotating frame propagated through 2070.

Venus or Mars, for example, can effectively filter out asteroids that do not come close to Earth from the set of nonrecoverable objects.

To further characterize the set of NEAs that are not recoverable, we investigate the evolution of the MOID of the 8051 nonrecoverable NEAs listed in Table 3. Analyzing the MOID of the nominal orbit is not sufficient in general, as large orbit uncertainties might admit orbit solutions with smaller values of the MOID. For each object, a total of 100 virtual asteroids are randomly sampled from the initial uncertainty distribution, their orbit is propagated for 100 years while monitoring the MOID at 1 day intervals, and the realizations with MOID < 0.001 au are recorded. This technique provides a rough estimate of the probability of the MOID becoming comparable to Earth's cross-section.

Table 6 summarizes the results from this experiment. From the set of asteroids with $H < 22$, 91% of the cases have zero samples reaching MOID < 0.001 au. When increasing the magnitude threshold to $H \leqslant 28$, the fraction of asteroids for which no samples reached the MOID threshold decreases to 85%.

4.2. Virtual Impactors

Of special interest are the asteroids from the Sentry risk list that are not recoverable. Particularly if there are virtual impactors (VI) with a significant impact probability, since these objects cannot be detected again except serendipitously, their orbits cannot be refined to rule out the impact trajectories. In total, there are 69 objects from the current Sentry risk list that are not recoverable in the next 50 years and that have virtual impactors with IP $> 10^{-5}$, 193 with IP $> 10^{-6}$, and 317 with IP $> 10^{-7}$. Table 7 contains the nonrecoverable asteroids with IP $> 10^{-5}$, indicating the date of close approach of the corresponding VI, the Palermo scale (PS) (Chesley et al. 2002), and the absolute magnitude. The median PS is -5.38.

Statistically, 41% of the 69 nonrecoverable asteroids with IP $> 10^{-5}$ might be recovered serendipitously by an all-sky survey in the next 50 years. The fraction goes down to 37% for asteroids with IP $> 10^{-6}$, and to 36% for asteroids with IP $> 10^{-7}$. These results indicate that a significant fraction of the objects on the Sentry risk list are bright enough to be detected and that it is their large orbit uncertainty that limits their targeted recovery.

Asteroids with large orbital uncertainty are more likely to admit orbit solutions that impact Earth. As a result, the orbital uncertainty of most asteroids on the Sentry risk list tends to be large and the main cause of asteroids admitting VIs being not recoverable is the growth of the plane-of-sky uncertainty.

5. Conclusions

Large orbit uncertainties can prevent an asteroid from being recovered by targeted observation campaigns. We find that the majority of known NEAs with $H < 22$ can be recovered by telescopes comparable to I52 (74% of the population) and to

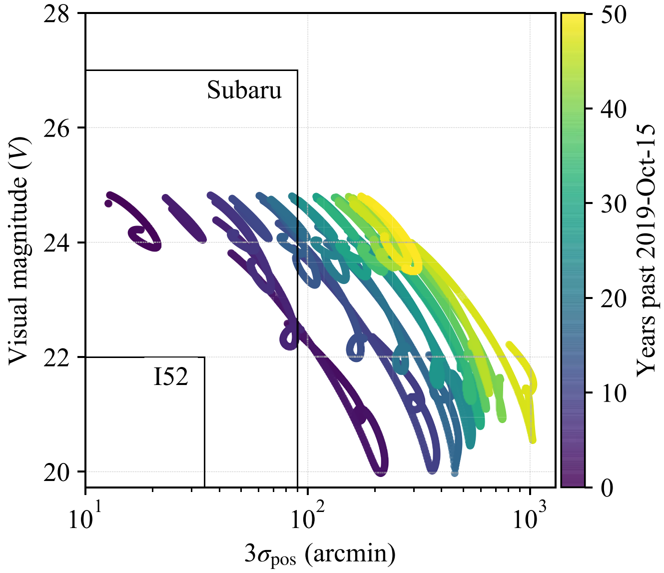

Figure 5. Time evolution of the plane-of-sky uncertainty and the visual magnitude of asteroid 2015 KC_{19}. Only the data points with $\varepsilon > 60°$ are shown.

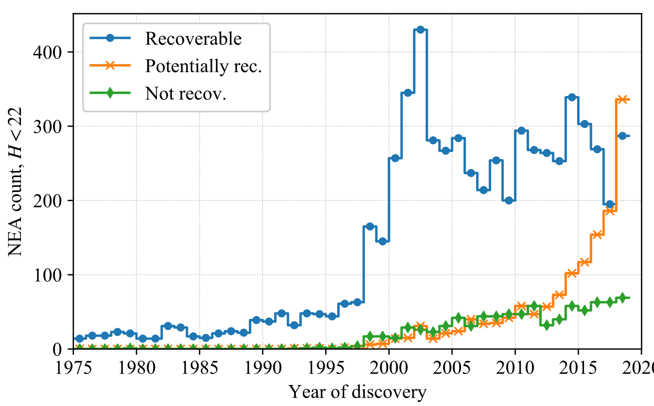

Figure 6. Number of recoverable, potentially recoverable, and nonrecoverable NEAs with $H < 22$ distributed by year of discovery.

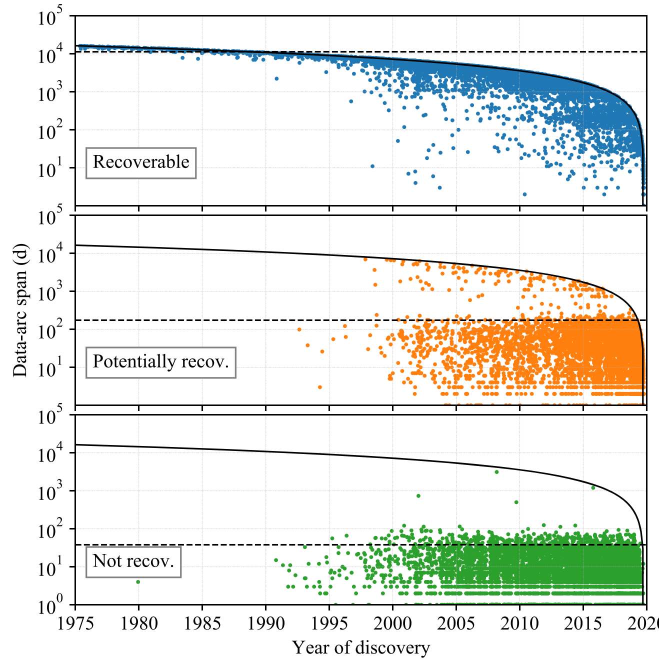

Figure 7. Data-arc span as a function of the year of discovery. The solid black line indicates the maximum possible length of the data arc and the dashed line is the 95th percentile.

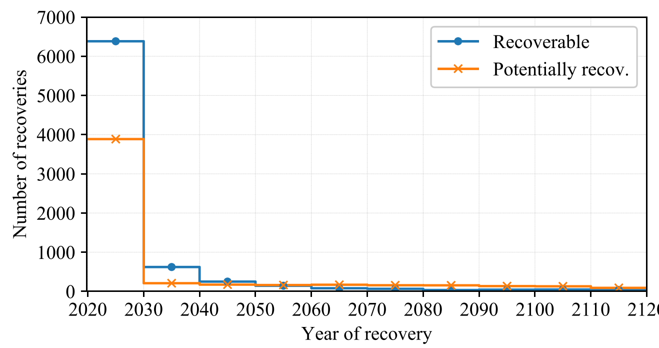

Figure 8. Distribution of recoveries by year.

Subaru's Hyper Suprime-Cam (up to 90% of the population), while only a small fraction (10%) of NEAs are not recoverable in the next 50 years under the conditions described in this paper. If we include all sizes down to approximately 10 m, about one-third of known NEAs are not recoverable. As for PHAs, only 7% cannot be recovered. Almost half of the low-MOID NEAs with $H \leqslant 28$ are not recoverable.

Asteroids on the Sentry risk list typically present large orbit uncertainties that are responsible for the relatively large fraction of objects that are not recoverable. In particular, there are 193 nonrecoverable asteroids with $H \leqslant 28$ that admit at least one virtual impactor with Earth-impact probability larger than 10^{-6}. Among the population of NEAs with $H < 22$, the probability of the MOID being less than 0.001 au is negligible in 91% of the cases.

Combining targeted recovery attempts with serendipitous detections from surveys can substantially reduce the fraction of asteroids that are not recoverable. A statistical analysis of the rate of detections by ongoing surveys suggests that up to 47% of all nonrecoverable NEAs could be recovered serendipitously in the next 50 years. More importantly, all-sky surveys might detect up to 43% and 37% of the low-MOID NEAs and asteroids on the Sentry risk list (respectively) that are not recoverable. Thus, surveys play an important role in complementing dedicated recovery efforts.

Follow-up observations are critical for recoveries, extending the span of the data arc to refine the orbit and to reduce the orbital uncertainty. In general, routine recoveries of asteroids observed at more than one apparition are usually possible, objects observed at a single apparition but for a relatively long period of time may be recovered with an aggressive campaign, whereas objects observed for just a few nights during a single apparition are typically not recoverable. Precoveries are particularly relevant in this context because they can potentially incorporate observations from multiple apparitions, increasing the chances of an asteroid being recoverable. The length of the data arc compared to the total number of available nights has been increasing consistently for asteroids discovered in recent years. Discovery statistics prove that the overall performance of the observational campaigns is improving provided that the number of discoveries keeps growing while the number of asteroids that are not recoverable remains approximately constant.

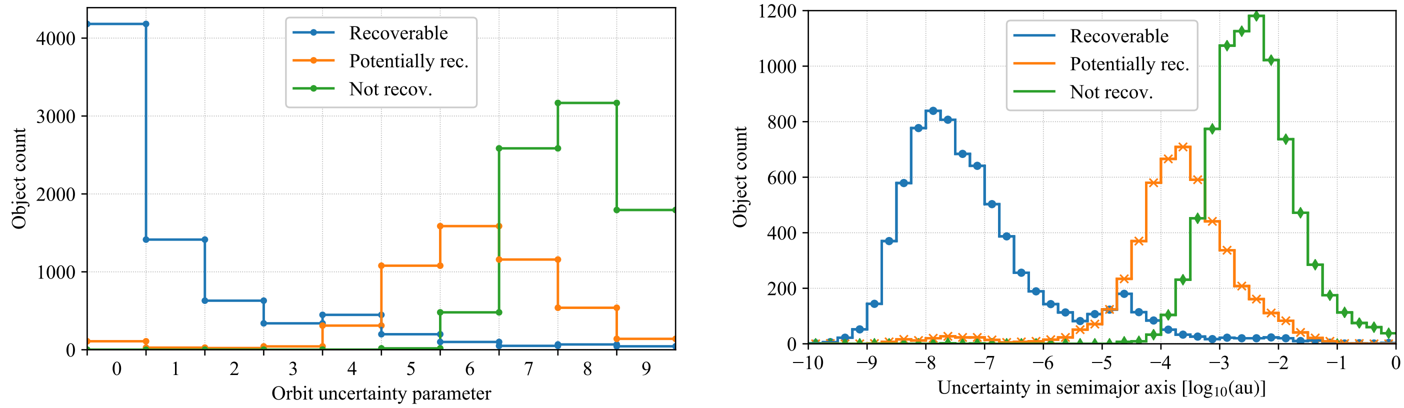

(a) Distribution by orbit uncertainty parameter U

(b) Distribution by uncertainty in semimajor axis

Figure 9. Distribution of recoverable, potentially recoverable, and nonrecoverable NEAs by orbit uncertainty.

Table 5
Statistical Estimate of Potential Serendipitous Recoveries by All-sky Surveys (a.s.) in the Next 50 Years

		Targeted Recovery	Recoverable by a.s.	
			Count	Fraction
NEAs	Recoverable	7474	7111	95.1%
	Potentially Recoverable	5014	3472	69.2%
	Not Recoverable	8051	3765	46.8%
	Total	20539	14348	69.9%
Low MOID	Recoverable	2349	2176	92.6%
	Potentially Recoverable	2531	1650	65.2%
	Not Recoverable	4617	1961	42.5%
	Total	9497	5787	60.9%
Sentry	Recoverable	9	9	100.0%
	Potentially Recoverable	129	82	63.6%
	Not Recoverable	193	71	36.8%
	Total	331	162	48.9%

Note. The numbers for targeted recoveries have been taken from Table 3. Percentages indicate the fraction of asteroids that can be detected by surveys relative to the total number of asteroids in each category.

Table 6
Fraction of Nonrecoverable Asteroids Organized by Absolute Magnitude and by the Probability of the MOID Being Less than 0.001 au

p(MOID $<$ 0.001 au)	$H < 22$	$H \leqslant 28$
0	90.7%	85.0%
(0,0.5)	6.6%	5.5%
[0.5,1)	1.5%	2.4%
1	1.2%	7.1%

The statistical results presented in this paper apply to the current snapshot of the database of known NEAs. In the future, as the number of known NEAs increases, the statistics may need to be updated to incorporate the new discoveries and reassess the performance of future follow-up efforts. Furthermore,

Table 7
Nonrecoverable Asteroids on the Sentry Risk List with IP $> 10^{-5}$ and $H \leqslant 28$, Sorted by Maximum Impact Probability

Designation	IP $\times 10^6$	C. A. Date	PS	H
2013 VW_{13}	292	2080-11-08.68	−4.09	26.2
2011 DU_9	279	2046-02-23.86	−4.22	26.7
2007 HB_{15}	263	2055-04-25.52	−4.94	27.7
2009 JF_1	259	2022-05-06.34	−3.28	27.1
2009 BE	220	2083-01-25.10	−4.32	26.1
2008 JL_3	146	2027-05-01.38	−3.27	25.4
2012 MF_7	132	2046-06-21.88	−4.62	26.9
2018 CM	112	2072-02-08.40	−5.41	27.8
2019 QR_3	112	2080-08-31.46	−5.09	27.1
2016 RR_1	99	2100-09-03.64	−5.72	28.0
2018 NW	85	2102-07-09.36	−5.38	27.8
2016 DK_1	73	2062-02-18.14	−5.36	27.5
1994 GK	68	2061-04-03.64	−3.66	24.2
2016 EM_{156}	55	2116-03-19.63	−6.06	27.9
2010 JH_{110}	52	2092-06-03.72	−5.19	26.3
2016 NL_{39}	50	2075-06-28.31	−5.82	27.6
2013 TP_4	49	2026-10-01.33	−4.43	27.3
2000 SB_{45}	48	2080-10-08.25	−4.24	24.5
2010 GH_7	48	2111-04-02.53	−5.92	27.3
2011 SM_{173}	48	2058-09-22.16	−5.51	27.8
2011 MX	44	2081-06-19.34	−5.37	26.9
2011 FQ_6	42	2075-03-23.98	−5.79	27.7
2010 CS_{19}	40	2104-02-13.66	−6.23	28.0
2019 JO_1	40	2052-04-28.09	−5.11	27.2
1994 GV	38	2101-04-12.54	−5.94	27.4
2016 CD_{30}	38	2070-01-31.72	−5.76	27.8
2008 CC_{71}	37	2066-02-27.51	−4.47	24.9
2005 QK_{76}	36	2030-02-26.34	−3.70	25.1
2010 UH	36	2115-07-14.48	−5.89	27.1
2011 SO_{189}	35	2087-09-24.84	−5.29	26.5
2011 EB_{74}	33	2054-03-16.51	−5.45	26.9
2013 GA_{55}	33	2114-04-06.04	−6.13	27.6
2013 FU_{13}	32	2088-03-12.92	−5.90	27.4
2005 TH_{50}	28	2077-10-02.75	−6.26	28.0
2011 EB	28	2077-02-27.32	−5.60	26.9
2013 EV_{27}	28	2038-02-28.99	−5.10	27.0
2015 BW_{516}	28	2061-01-29.82	−5.76	27.4
2016 GK_2	28	2096-03-26.73	−6.17	27.7
2019 KL	27	2047-05-26.14	−4.95	26.4
2012 VE_{77}	26	2033-11-17.53	−4.59	26.3
2007 CC_{27}	24	2088-02-12.61	−5.70	27.0
2012 BU_1	24	2102-01-14.38	−6.23	27.7

Table 7
(Continued)

Designation	IP × 10^6	C. A. Date	PS	H
2007 DX_{40}	22	2056-08-18.22	−4.26	24.6
2009 BF_{58}	22	2083-01-22.22	−6.00	27.3
2019 GD_4	22	2084-02-03.93	−6.21	27.7
2014 GN_1	21	2061-09-16.84	−4.17	24.6
2017 GG_8	21	2066-03-31.51	−5.19	26.1
2007 VE_8	20	2062-11-06.12	−4.96	25.4
2009 WP_6	20	2074-11-16.41	−5.25	26.8
2011 OB_{26}	20	2115-08-11.97	−5.24	25.6
2011 UM_{169}	20	2102-10-24.52	−4.88	25.0
2014 QC_{391}	20	2100-09-07.25	−6.24	27.4
2015 WN_1	20	2092-11-11.94	−5.59	26.5
2010 VW_{194}	19	2079-11-12.83	−5.66	26.5
2012 EK_5	18	2095-03-24.49	−5.09	25.6
2019 JR_2	17	2114-05-01.79	−5.97	27.0
2013 BL_{18}	15	2086-01-14.31	−5.36	25.9
2004 PU_{42}	14	2085-08-17.06	−5.89	26.7
2010 GM_{23}	14	2105-04-15.16	−4.88	24.7
2011 ES_4	14	2055-09-02.70	−5.20	25.7
2014 OX_3	14	2116-07-24.74	−6.42	27.8
2019 BZ	14	2078-07-28.29	−6.26	27.6
2018 RB_2	13	2102-09-06.59	−6.30	27.3
2005 XA_8	12	2069-12-05.99	−5.25	25.7
2011 AE_3	12	2023-01-03.19	−5.70	28.0
2012 BA_{77}	12	2065-10-09.82	−5.30	25.8
2013 BR_{27}	11	2092-01-17.10	−6.46	27.8
2007 KE_4	10	2029-05-26.02	−4.52	25.2
2010 JL_{88}	10	2082-05-18.89	−5.87	26.8

undiscovered NEAs generally present unfavorable observation conditions, likely due to being close to resonances. Thus, the fraction of NEAs that are recoverable, potentially recoverable, and not recoverable may change when discovering more asteroids trapped in such dynamical regimes.

This work was carried out at the Jet Propulsion Laboratory, California Institute of Technology, under a contract with the National Aeronautics and Space Administration. We thank Peter Vereš (MPC) and Tim Spahr for their valuable comments and their feedback about this manuscript.

ORCID iDs

Javier Roa https://orcid.org/0000-0002-0810-1549
Davide Farnocchia https://orcid.org/0000-0003-0774-884X
Steven R. Chesley https://orcid.org/0000-0003-3240-6497
Ryan S. Park https://orcid.org/0000-0001-9896-4585
Shantanu P. Naidu https://orcid.org/0000-0003-4439-7014

References

Boattini, A., D'Abramo, G., Valsecchi, G., & Carusi, A. 2007, EM&P, 100, 31
Christensen, E. J. 2019, in Planetary Defense Conf. 2019, ed. W. Ailor (Washington, DC: IAA)
Chesley, S. R., Chodas, P. W., Milani, A., Valsecchi, G. B., & Yeomans, D. K. 2002, Icar, 159, 423
Chesley, S. R., Farnocchia, D., Nolan, M. C., et al. 2014, Icar, 235, 5
Damour, T., & Deruelle, N. 1985, AIHS, 43, 107
Farnocchia, D., Chesley, S., Milani, A., Gronchi, G., & Chodas, P. 2015, in Asteroids IV, ed. P. Michel, F. E. DeMeo, & W. F. Bottke (Tucson, AZ: Univ. Arizona Press), 815
Farnocchia, D., & Chesley, S. R. 2014, Icar, 229, 321
Farnocchia, D., Chesley, S. R., Chodas, P. W., et al. 2013, Icar, 224, 192
Folkner, W. M., Williams, J. G., Boggs, D. H., Park, R. S., & Kuchynka, P. 2014, IPNPR, 196, 1
Granvik, M., Morbidelli, A., Jedicke, R., et al. 2016, Natur, 530, 303
Harris, A. W., & D'Abramo, G. 2015, Icar, 257, 302
Jones, R. L., Slater, C. T., Moeyens, J., et al. 2018, Icar, 303, 181
Ivezić, Ž, Kahn, S. M., Tyson, J. A., et al. 2019, ApJ, 873, 111
Kaiser, N., Aussel, H., Burke, B. E., et al. 2002, Proc. SPIE, 4836, 154
Mainzer, A. 2006, BAAS, 38, 568
Mainzer, A., Grav, T., Bauer, J., et al. 2011, ApJ, 743, 156
Milani, A., Chesley, S. R., & Valsecchi, G. B. 2000, P&SS, 48, 945
Miyazaki, S., Komiyama, Y., Nakaya, H., et al. 2012, Proc. SPIE, 8446, 84460Z
Morrison, D. 1992, The Spaceguard Survey: Report of the NASA International Near-Earth-Object Detection Workshop, Tech. Rep. NAS 1.15:107979, https://ntrs.nasa.gov/api/citations/19920025001/downloads/19920025001.pdf
Ostro, S. J., Hudson, R. S., Benner, L. A., et al. 2002, in Asteroids III, ed. W. F. Bottke, Jr. et al. (Tucson, AZ: Univ. Arizona Press), 151
Ramanjooloo, Y., Wainscoat, R. J., Weryk, R., Chambers, K. C., & Magnier, E. A. 2018, DPS Meeting, 50, 304.08
Stokes, G. H., Barbee, B., Bottke, W., et al. 2017, Update to determine the feasibility of enhancing the search and characterization of NEOs, Rep. of the Near-Earth Object Science Definition Team, https://cneos.jpl.nasa.gov/doc/2017_neo_sdt_final_e-version.pdf
Stokes, G. H., Evans, J. B., Viggh, H. E., Shelly, F. C., & Pearce, E. C. 2000, Icar, 148, 21
Stuart, J. S., & Binzel, R. P. 2004, Icar, 170, 295
Tholen, D. 2003, BAAS, 35, 972
Tricarico, P. 2017, Icar, 284, 416
Vereš, P., Farnocchia, D., Chesley, S. R., & Chamberlin, A. B. 2017, Icar, 296, 139
Vokrouhlický, D., Farnocchia, D., Čapek, D., et al. 2015, Icar, 252, 277
Vokrouhlický, D., Milani, A., & Chesley, S. 2000, Icar, 148, 118
Ye, Q., Masci, F. J., Ip, W.-H., et al. 2020, AJ, 159, 70